



# Development of a ground level enhancement alarm system based upon neutron monitors

T. Kuwabara,<sup>1</sup> J. W. Bieber,<sup>1</sup> J. Clem,<sup>1</sup> P. Evenson,<sup>1</sup> and R. Pyle<sup>1</sup>

Received 23 January 2006; revised 11 April 2006; accepted 12 April 2006; published 11 October 2006.

[1] We have developed a system that watches for count rate increases recorded in real time by eight neutron monitors, which triggers an alarm if a ground level enhancement (GLE) is detected. In this work, we determine optimal strategies for detecting the GLE event at a very early stage, while still keeping the false alarm rate at a very low level. We study past events to optimize appropriate intensity threshold values and a baseline to determine the intensity increase. The highest-level alarm, which we term an “alert,” is generated when a 4% increase is recorded at three stations in 3 min averaged data. At this level, the false alarm rate obtained by backtesting over the past 4.4 years is zero. Ten GLEs occurred in this period, and our system produced GLE alarms for nine events. Alarm times for these nine events are compared with satellite proton data. The GLE alert precedes the earliest alert from GOES (100 MeV or 10 MeV protons) by  $\sim 10$ –30 min. Real-time GLE data may be viewed at <http://neutronm.bartol.udel.edu/spaceweather>. An automated e-mail alert system is under development.

**Citation:** Kuwabara, T., J. W. Bieber, J. Clem, P. Evenson, and R. Pyle (2006), Development of a ground level enhancement alarm system based upon neutron monitors, *Space Weather*, 4, S10001, doi:10.1029/2006SW000223.

## 1. Introduction

[2] Solar energetic particles (SEPs) produced and accelerated at a solar eruptive event can propagate to Earth, causing damage to satellite electronics, and posing a radiation hazard to astronauts and air crews. When primary SEPs (predominantly protons) with sufficient energy (>500 MeV) and intensity hit Earth’s atmosphere, a ground-based neutron monitor records an intensity increase of secondary neutrons, resulting in a ground level enhancement (GLE). Since SEPs generally have soft energy spectra, most damage in space is caused by lower-energy particles that are not detected by ground-based neutron monitors. Virtually all GLEs are accompanied by major solar energetic particle (SEP) events at lower energy. Because the GLE particles have large mean free paths and travel almost at the speed of light, a GLE alarm can provide a very useful early warning of an impending solar radiation storm. (At times, however, a serious space radiation event is not accompanied by a GLE.) For air crews, GLEs are the events of principal concern [Wilson *et al.*, 2003], because the associated primary SEPs possess sufficient energy to raise secondary radiation levels at aircraft altitudes. Thus a GLE alarm is of direct relevance to pilots and air crews, especially those flying the increasingly

popular polar routes from the United States to Asia, where Earth’s magnetic field provides very little shielding.

[3] Though the flux of particles at GLE energies is small, they can be detected with high accuracy by detectors with large volume such as ground-based neutron monitors. A sample SEP event is shown in Figure 1 [Bieber *et al.*, 2004]. The start time of the intensity increase in neutron monitors (bottom plot) is earlier than that of the low-energy proton flux (top plot). Furthermore, the flux increase is smaller at neutron monitor energies (though detected with higher accuracy), and time to reach maximum intensity is shorter for neutron monitors. Consequently, our GLE observation makes it possible to warn of the arrival of SEPs earlier than methods based upon lower-energy charged particles detected by satellites. Moreover, neutron monitor observations are the only way to identify the occurrence of SEP event on the ground, and would be available even if satellite data were not readily available.

[4] The University of Delaware provides real-time displays of the cosmic ray intensity of several ground-based neutron monitors with excellent statistics and 1 min time resolution (Bartol Research Institute Web site at the University of Delaware, 2006, available at <http://neutronm.bartol.udel.edu/spaceweather>). This article describes the development of a system that watches for count rate increases recorded in real time in these data, which triggers an alarm if a GLE is detected. We determine optimal strategies for detecting the GLE event at a very

<sup>1</sup>Bartol Research Institute and Department of Physics and Astronomy, University of Delaware, Newark, Delaware, USA.

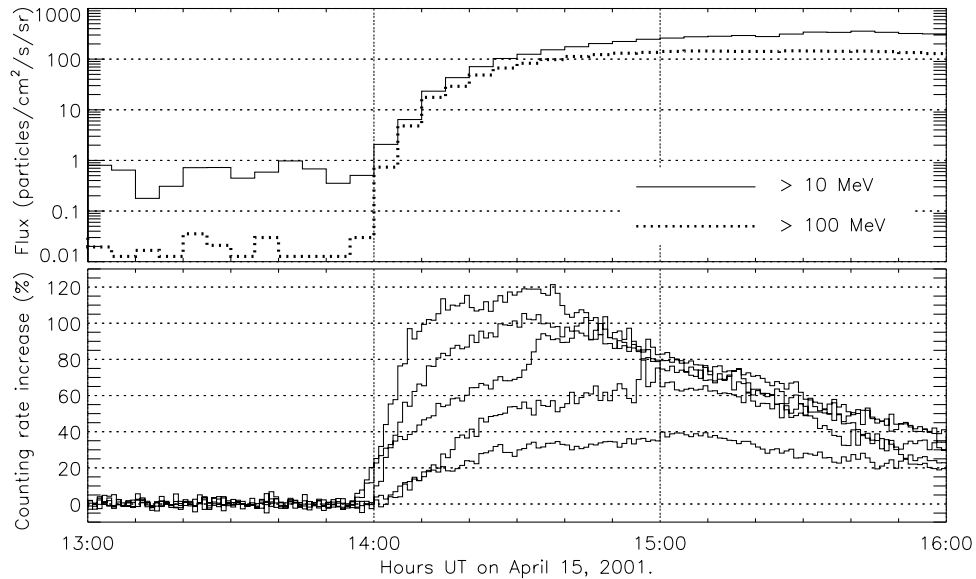


**Figure 1.** SEP event on 15 April 2001: (top) low-energy proton integral flux recorded by the GOES 10 satellite (solid line, >10 MeV and dotted line, >100 MeV) and (bottom) 1 min average of neutron rates detected in several neutron monitors. Note that the neutron monitor onset clearly precedes the GOES onset.

early stage, while still keeping the false alarm rate at a very low level. We study past events to optimize appropriate intensity threshold values and a baseline to determine the intensity increase. Using the strategies derived in this paper, we backtest the GLE alarm system on nine recent GLEs, and we consider the rate of false alarms. Because the onset of SEPs are regularly monitored by the GOES satellite, and alerts are issued by e-mail and on the Web by the NOAA Space Environment Center (NOAA Space Environment Center Web site, 2006, available at <http://www.sec.noaa.gov>), we compare the issue times of NOAA SEC alerts with the GLE alarm times to determine how useful our system is.

## 2. Data and Events

[5] This study uses data recorded by eight neutron monitors operated by the University of Delaware. Basic

station information appears in Table 1. Since these stations are located at high geomagnetic latitude, they have greater sensitivity to the lower end of the neutron monitor energy range than do midlatitude or low-latitude stations, an important factor considering the typical soft spectrum of SEPs. Moreover, the two detectors at South Pole (standard neutron monitor and unshielded detector) are located at 2820 m and thus have even greater sensitivity to low-energy primary particles because of the low atmospheric absorption of the secondary neutrons generated near the top of the atmosphere. Owing to these factors, these stations are well suited to detect the occurrence of a GLE rapidly and accurately.

[6] Pressure corrected 1 min data from each of the stations listed in Table 1 are available in real time for at least part of the day. In the case of the South Pole detectors, real-time data are available in a variable time window depending upon communications satellite visibil-

**Table 1.** Information on the Eight Neutron Monitors Used in This Work<sup>a</sup>

Station	Type	Count Per Hour	Latitude, deg	Longitude, deg	Altitude, m
Inuvik, Canada	18NM64	$6.6 \times 10^5$	68.4 N	133.7 W	21
Fort Smith, Canada	18NM64	$7.4 \times 10^5$	60.0 N	111.9 W	203
Peawanuck, Canada	18NM64	$7.3 \times 10^5$	55.0 N	85.4 W	52
Nain, Canada	18NM64	$7.3 \times 10^5$	56.5 N	61.7 W	46
Thule, Greenland	18NM64	$8.0 \times 10^5$	76.5 N	68.7 W	44
McMurdo, Antarctica	18NM64	$9.4 \times 10^5$	77.9 S	166.6 E	48
South Pole, Antarctica	3NM64	$10.3 \times 10^5$	90.0 S	0.0 E	2820
South Pole Bares	6NM64	$3.2 \times 10^5$	90.0 S	0.0 E	2820

<sup>a</sup>Station name, detector type, average count rate (at 2005), geographical latitude, longitude, and altitude are listed. South Pole is a standard 3NM64, while South Pole Bares is our "Polar Bare," a 6NM64 (3NM64 until 20 January 2004) without the usual lead shielding. It responds to a slightly lower energy primary cosmic ray than the standard monitor.

**Table 2.** Ground Level Enhancements During the Analysis Interval<sup>a</sup>

Event Date	Flare Onset, UT	Location	Type
14 Apr 2001	1319	S20W85	2B/X14.4
18 Apr 2001	0211	S20WLimb <sup>b</sup>	C2
4 Nov 2001	1603	N06W18	3B/X1.0
26 Dec 2001	0432	N08W54	1B/M7.1
24 Aug 2002	0049	S02W81	1F/X3.1
28 Oct 2003	0951	S16E08	4B/X17.2
29 Oct 2003	2037	S15W02	2B/X10.0
2 Nov 2003	1703	S14W56	2B/X8.3
20 Jan 2005	0636	N14W61	2B/X7.1

<sup>a</sup>Event date, X-ray flare onset time given by GOES, location, and importance of the associated X-ray flare are listed.

<sup>b</sup>Associated X-ray flare occurred behind the limb.

ity. Recent  $\sim 5$  year data observed from October 2000 to May 2005 are analyzed in this work. During this period ten GLE events occurred, and we use nine events listed in Table 2. One event that occurred on 17 January 2005 is excluded from this work because the intensity increase was only 2% at South Pole station. We employ these nine events to determine optimal parameters for use in a GLE alarm system, and we also employ these events for back-testing the system and determining its performance in relation to presently available SEP alarms.

### 3. Algorithm for Issuing an Alarm

[7] We define three levels of alarm (watch, warning, and alert) on the basis of the number of stations that record a significant intensity increase. As illustrated in Figure 2, we set a threshold level  $I_{th}$  for the cosmic ray intensity increase, and we generate an alarm when the number of stations that exceed the threshold level is 1 for watch, 2 for warning, and 3 for alert. Setting the threshold level  $I_{th}$  requires a tradeoff between generating the earliest possible alarm (which favors a lower threshold) and avoiding false alarms (which favors a higher threshold). Desired properties of the false alarm rate for the different levels of alarm are presented in Table 3. Though our data are observed in 1 min resolution, it may be desirable to average 2 or more minutes of data in order to avoid the influence of statistical noise [Dorman *et al.*, 2003]. More-

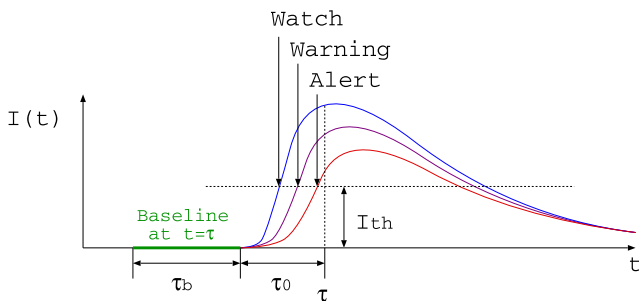


**Figure 2.** Condition for issuing three levels of alarm. Intensity increases recorded at three stations during a typical (notional) GLE are illustrated.

over, sometimes real-time data tend to include data anomalies resulting from data transmission errors, but such anomalies were removed from the data used in this work. Because anomalies are often limited to a single minute of data, averaging several minutes together can reduce their effect in the real-time processing. (We do not archive the real-time data; hence we are unable to repeat this study with anomalies included. However, large anomalies ( $>30\%$ ) are automatically detected and removed in our real-time system. The remaining small anomalies are sufficiently rare,  $\leq 1$  per day per station, that the rate of false alarms from coincident anomalies is negligible at the warning and alert level.)

[8] The count rate increase due to SEPs during a GLE is usually shown as the percentage deviation from a preevent baseline count rate due to Galactic cosmic rays. However, because we are developing a system to detect GLEs in real time, an automated method to compute the baseline is required. Since the observed count rate has statistical fluctuations, a large enough time period should be chosen to determine an accurate baseline. In addition, it is desirable to set the end of the baseline interval at some time earlier than the current time. This is because as illustrated in Figure 2, the count rate increase during the GLE should be calculated from a baseline that does not include the period when SEPs are present, at least until the intensity increase is well recognized.

[9] By using a trailing moving average value for the current count rate, the intensity at time  $t = \tau$  is calculated each minute from the observed count rate  $N(t)$  averaged over the preceding  $\tau_c$  minutes, and expressed as a percentage of the baseline defined as described above, i.e.,

$$I(\tau) = \left\{ \frac{1}{\tau_c} \sum_{t=\tau-\tau_c}^{\tau} N(t) \right\} / \left\{ \frac{1}{\tau_b} \sum_{t=\tau-\tau_0-\tau_b}^{\tau-\tau_0} N(t) \right\}, \quad (1)$$

where  $\tau_c$  is the averaging time,  $\tau_b$  is the duration of the baseline and  $\tau_0$  is the time interval between the baseline and current time. In Appendix A, the method for determining the optimum values of  $\tau_c$ ,  $\tau_b$ ,  $\tau_0$  and  $I_{th}$  is explained. These values are determined from past events as  $\tau_c = 3$  min,  $\tau_b = 75$  min,  $\tau_0 = 10$  min and  $I_{th} = 4\%$ .

### 4. Comparison With GOES Proton Data

[10] In this section, we compare the GLE alarm times to alarm times on the basis of satellite proton data. The

**Table 3.** Definition and Characteristics of Three Alarm Levels

Type of Alarm	Station Number <sup>a</sup>	Expected Occurrence Rate
Watch	1	Many false alarms
Warning	2	A few false alarms
Alert	3	Zero or near-zero false alarms

<sup>a</sup>Number of stations that exceed the threshold value.

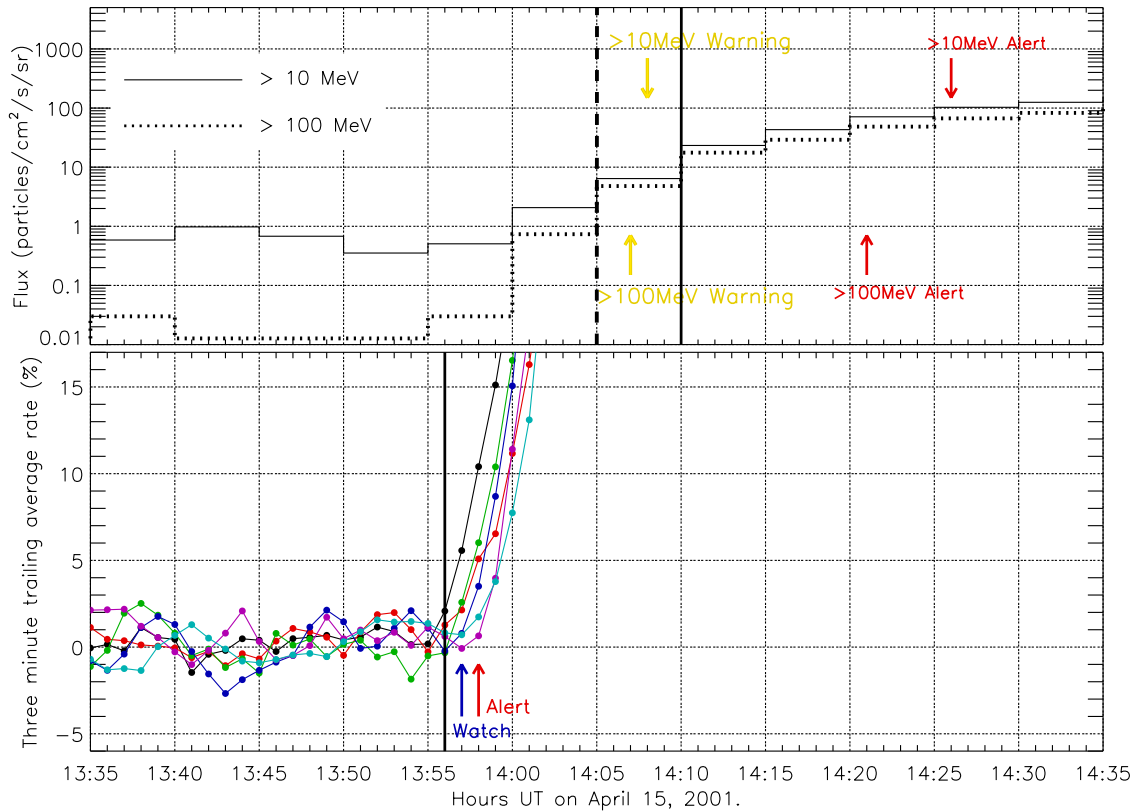


**Figure 3.** (top) Proton flux and (bottom) cosmic ray intensity from neutron monitors for the GLE event on 15 April 2001. In the top plot, the solid line and dotted lines show the GOES  $>10$  MeV and  $>100$  MeV integral proton data, respectively. In the bottom plot, 3 min trailing moving average rates at six neutron monitor stations are plotted. Vertical lines drawn in both plots also show the onset time of SEP event ( $>10$  MeV, solid line and  $>100$  MeV, dotted line) and GLE. Arrows indicate the time when each alarm is issued (proton monitor) or generated (neutron monitor). The colors of the arrows represent alarm levels (blue, watch; yellow, warning; and red, alert).

NOAA Space Environment Center (NOAA/SEC) provides real-time monitoring of the proton flux observed by the GOES satellite during many solar and geophysical events, and issues alarms on the Web and via e-mail (NOAA Web site, <http://www.sec.noaa.gov>). Two energy channels of data ( $>10$  MeV and  $>100$  MeV) and two levels of alarm (warning and alert) are issued during SEP events. A warning message is issued when a flux level above 10 particle flux unit (pfu) is predicted at  $>10$  MeV or when greater than 1 pfu is predicted for  $>100$  MeV. (Note that the SEC's use of the term "warning" is rather different from our usage for the GLE alarm, as it is a prediction rather than an actual detection of SEP.) An alert message is issued when a flux level exceeding 10, 100, 1,000, 10,000, or 100,000 pfu is confirmed at  $>10$  MeV, or when greater than 1 pfu is confirmed at  $>100$  MeV. Issue times of the alarms can be used as a barometer of how fast an SEP event is detected in low-energy proton data, therefore we compare our alarm time with these issue times. (We observe that an SEC alert is typically not issued till some

minutes after the relevant threshold is crossed, however we consider the issue time of an alert to be the relevant one for this comparison.)

[11] Figure 3 shows the flux increase of the GOES proton monitor and the count rate increase of several neutron monitors for the 15 April 2001 event. In the top plot, the solid line and dotted line show the  $>10$  MeV and  $>100$  MeV integral proton flux respectively. Shown in the bottom plot are 3 min trailing moving average rates,  $I(\tau)$ , calculated by equation (1) from recorded count rates,  $N(\tau)$ , at six neutron monitor stations. Vertical lines drawn in each plot also show the onset time of the SEP event (solid line,  $>10$  MeV flux exceeds 10 pfu and dotted line,  $>100$  MeV flux exceeds 1 pfu) and GLE (1 min cosmic ray count rate exceeds 3% intensity threshold). Some arrows in Figure 3 indicate the time when each alarm is issued (proton monitor) or generated (neutron monitor). The color of the arrows represents alarm levels (blue, watch; yellow, warning; and red, alert). From Figure 3, it is clear that each level of alarm produced in our system is faster than the issue time from

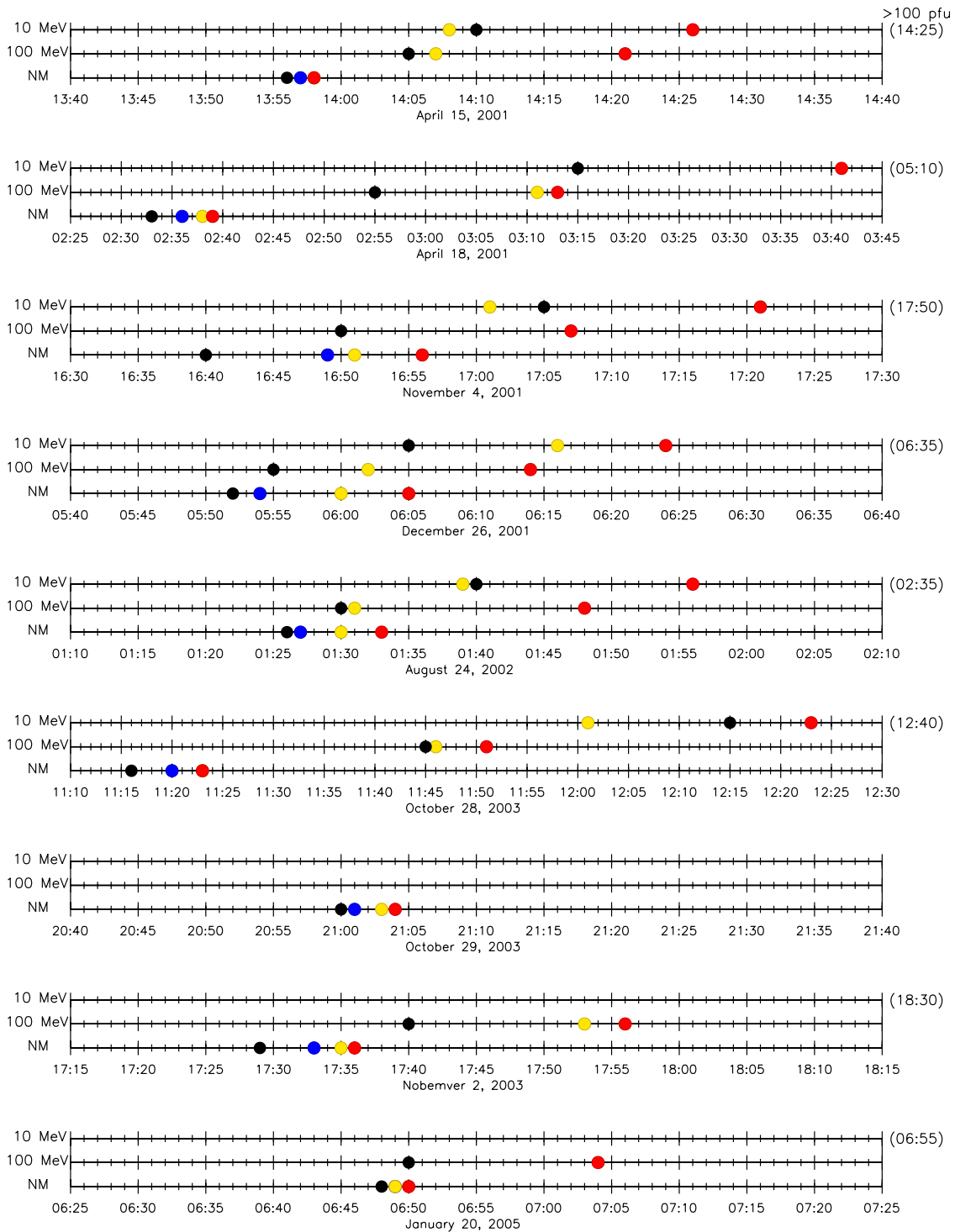
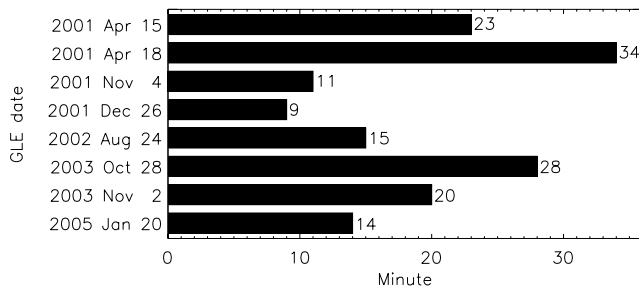


Figure 4. Comparison between the alert times from our system with alarm issue times from proton data at SEC/NOAA for nine GLE events. Colored points on the time axis show the onset time of events and alarm timings for each energy (black, event onset; blue, watch; yellow, warning; and red, alert). Times written on the right of the 10 MeV axis show the times when particle flux exceeded 100 pfu (moderate storm level). Note that the total time interval plotted is different for each event.



**Figure 5.** Number of minutes by which GLE alert precedes earliest SEC proton alert.

SEC/NOAA, and the GLE alarm times precede the event onset of the GOES protons. Moreover, the proton flux observed in the  $>10$  MeV channel exceeds 100 pfu at 1425 UT. This flux level is defined as a “moderate storm” (S2 on NOAA Space Weather Scale for Solar Radiation Storms (NOAA Web site, <http://www.sec.noaa.gov>)) that has the possibility to cause single-event upsets aboard satellites. Both our system and the SEC/NOAA ( $>100$  MeV proton) system can produce alarms before the beginning of the moderate storm, but alarm times in this event are 27 min before the storm beginning for neutron monitors and only 4 min for  $>100$  MeV proton.

[12] In Figure 4 alarm times from our system for nine GLE are compared with alarm issue times from GOES proton data. Colored points on the time axis are coded the same as arrows in Figure 3, and black points show the event onset time for each energy. For the proton data in three events, 29 October 2003 ( $>10$  MeV and  $>100$  MeV), 2 November 2003 ( $>10$  MeV), and 20 January 2005 ( $>10$  MeV), there is no well-defined onset, warning, or alert, because the proton flux was already above the threshold value (10 pfu at  $>10$  MeV, and 1 pfu at  $>100$  MeV) from a prior event. We see that the GLE alert preceded the earliest alert from GOES ( $>100$  MeV or  $>10$  MeV) by  $\sim 10$ –30 min in all events, as shown also in Figure 5. Also from Figure 4, we see that nearly half of all events had the property (like the 15 April 2001 event) that the GLE alert time preceded the onset of the GOES proton event. Moreover, times written on the right of the 10 MeV axis show the time when particle flux exceeds 100 pfu, thus qualifying as a “moderate storm.” GLE alerts preceded the beginning of the moderate storm by times ranging from  $\sim 5$  to 150 min, the average (omitting the 29 October 2003 GLE where a storm was already in progress) being 60 min. In several events such as 15 April 2001 and 20 January 2005, the GLE alert provided a much earlier alarm prior to the beginning of the moderate storm than the SEC/NOAA alert.

[13] Finally, we discuss the occurrence rate of GLEs versus SEP events, because there are some SEP events that are not accompanied by GLE. From the GOES satellite, a total of 29 events for which particle flux exceeded 100 pfu was observed at  $>10$  MeV channel

during this period. These events are listed in Table 4, and are classified by maximum proton flux as S2 (moderate,  $>100$  pfu), S3 (strong,  $>1000$  pfu), and S4 (severe,  $>10,000$  pfu). Eight of nine GLE events accompanied SEP events, and are marked in the right column. An event that occurred on 20 January 2005 was originally not an individual SEP event, because a former event on 16 January was continuing when this event occurred. However, we consider this as a separate SEP event because particle flux at  $>10$  MeV was lower than 100 pfu before event onset, and it clearly increased to  $>1000$  pfu. On the other hand, another SEP event that was accompanied by GLE occurred on 29 October 2003 but is excluded in Table 4 because particle flux was already  $>1000$  pfu before GLE onset and further particle increase after GLE onset was small. From Table 4, we can confirm that all GLEs except for 29 October 2003 event accompanied S2 or greater storms. The occurrence rate of GLEs is 29% at S2 or greater storm, 36% at S3 or greater storm,

**Table 4.** List of the SEP Events During the Analysis Period<sup>a</sup>

Year	Start Time, UT	Maximum Time, UT	Flux	GLE
<i>S4 Severe</i>				
2001	4 Nov 1705	6 Nov 0215	31,700	yes
2003	28 Oct 1215	29 Oct 0615	29,500	yes
2001	22 Nov 2320	24 Nov 0555	18,900	
2000	8 Nov 2350	9 Nov 1555	14,800	
2001	24 Sep 1215	25 Sep 2235	12,900	
<i>S3 Strong</i>				
2005	16 Jan 0210	17 Jan 1750	5,040	
2002	21 Apr 0225	21 Apr 2320	2,520	
2001	1 Oct 1145	2 Oct 0810	2,360	
2004	25 Jul 1855	25 Jul 1855	2,086	
2005	–	20 Jan 0810	1,860	yes <sup>b</sup>
2003	2 Nov 1105	3 Nov 0815	1,570	yes
2001	2 Apr 2340	3 Apr 0745	1,110	
<i>S2 Moderate</i>				
2001	15 Apr 1410	15 Apr 1920	951	yes
2000	4 Nov 1520	26 Nov 2030	940	
2002	22 May 1775	23 May 1055	820	
2001	26 Dec 0605	26 Dec 1115	779	yes
2004	7 Nov 1910	8 Nov 0115	495	
2001	16 Aug 0135	16 Aug 0355	493	
2003	26 Oct 1825	26 Oct 2235	466	
2002	9 Nov 1920	10 Nov 0540	404	
2001	10 Apr 0850	11 Apr 2055	355	
2003	4 Nov 2225	5 Nov 0600	353	
2001	18 Apr 0315	18 Apr 1045	321	yes
2002	24 Aug 0140	24 Aug 0835	317	yes
2004	13 Sep 2105	14 Sep 0005	273	
2002	16 Jul 1750	17 Jul 1600	234	
2002	7 Sep 0440	7 Sep 1650	208	
2003	28 May 2335	29 May 1530	121	
2001	30 Dec 0245	31 Dec 1620	108	

<sup>a</sup>The 29 events for which particle flux reached more than 100 pfu in  $>10$  MeV channel are listed in order of ascending maximum particle flux. Eight GLE events that accompanied SEP events are marked in the right column. (One GLE is omitted because a radiation storm was already in progress at event onset; see text.)

<sup>b</sup>See text for details about this event.

and 40% at S4 storm; that is, GLE tend to occur more frequently in higher-level storms.

## 5. Role of South Pole Neutron Monitor

[14] The GLE alarm system described above is only partially realizable at present, because the South Pole neutron monitor and bare counter closed on 22 November 2005. Even while it was operating, real-time data transmission from South Pole was limited to the few hours a day (as of 2005) when a large bandwidth communications satellite was accessible from the station. However, our backtesting study employed the data as though they were available full time in real time, as they would be in an operational system with appropriate priority to utilize the continuous, low bandwidth iridium connection to the station.

[15] The South Pole neutron monitor was the world's most sensitive detector of solar cosmic rays, because it was the only monitor at a location that is both high latitude (effectively zero geomagnetic cutoff) and high altitude. In addition, the monitor and bare counter can be treated as two independent stations in a GLE alarm system, provided their supporting data acquisition systems are sufficiently separate. To assess the impact of the closure of these instruments, we repeated the backtesting study of the preceding section with the South Pole neutron monitor and bare counter omitted. For one event, this omission resulted in no GLE alert being issued at all. For the remaining eight events, the time that a GLE alert was issued increased by an average of 8 min, with the maximum increase being 26 min for the event of 29 October 2003. Correspondingly, the average lead time of the GLE alert relative to the earliest GOES alert decreased from 19 min to 11 min when South Pole is omitted.

[16] In order to implement fully the GLE alert system described here, the South Pole neutron monitor and bare counter would have to be reopened, and priority access to the iridium communication link to South Pole would have to be authorized to permit full-time connectivity. An alternative possibility would be to deploy another neutron monitor and bare counter combination at a different high-latitude, high-altitude location (e.g., the mountains of Alaska) where full-time communications is feasible. It is also likely that having detectors in the Arctic and Antarctic simultaneously returning data would provide superior performance to having either in isolation.

## 6. Summary

[17] We have developed a real-time GLE detection system using eight high-latitude neutron monitors that have sensitivity to relativistic SEPs. To reduce fluctuations and accurately detect the GLE, we calculate the intensity increase from a 3 min moving average counting rate relative to a 75 min baseline extending from 85 min to 10 min before the current time. GLE alarms are produced at three levels (watch, warning, and alert) corresponding

to the number of stations that exceed the intensity threshold. The intensity threshold is set to 4% on the basis of examination of false alarm rates as well as elapsed time between event onset and generation of an alarm. All these parameters (baseline, threshold, etc) were optimized by backtesting against past neutron monitor data.

[18] During the 4.4-year period of our backtesting study, the false alarm rate for watch, warning, and alert was  $\sim 40/\text{yr}$ , less than  $1/\text{yr}$ , and  $0/\text{yr}$  respectively. Ten GLE events were occurred in this period, and our system produced GLE alarms for nine events, and missed one event. Alert times decided from this algorithm were compared with the earliest alert issued by SEC/NOAA on the basis of GOES (100 MeV or 10 MeV protons) data. We find that alert times produced by our system are  $\sim 10\text{--}30$  min earlier than alert issue times from SEC/NOAA, and are also substantially earlier ( $\sim 60$  min) than the time when dangerous amounts of low-energy particles reach the satellite (S2 storm level). These results suggest that our system can provide valuable added minutes of advance warning for radiation events of concern for satellites, astronauts, and air crews. We are presently developing an automated system to send out GLE alarms by e-mail when a possible GLE is detected.

## Appendix A: Determination of Parameters

[19] In this section, we optimize the appropriate values of  $\tau_c$ ,  $\tau_b$ ,  $\tau_0$  and  $I_{th}$  that define intensity threshold and a baseline to determine the intensity increase.

### A1. Define the Baseline

[20] Two parameters,  $\tau_b$  and  $\tau_0$ , that define the baseline are determined in this subsection. We determine optimal values for these parameters by setting  $\tau_b$  sufficiently large to produce an acceptably small level of fluctuations in the Galactic cosmic ray background intensity, and by determining a suitable separation  $\tau_0$  of the baseline interval from the evaluation time. We calculate the standard deviation of the quantity  $I(\tau)$  defined in equation (1) for the past  $\sim 5$  years of data for all stations. One minute counting rates are used for this calculation (i.e., we temporarily set  $\tau_c = 1$  min), and time periods when GLE events are observed are removed. The left plot in Figure A1 displays this standard deviation for  $\tau_0 = 1\text{--}30$  min and  $\tau_b = 20\text{--}150$  min. The standard deviation becomes small at  $\tau_b = 75$  min for all  $\tau_0$ . The deviation is larger at small  $\tau_b$  because of increased statistical noise, and it is larger at large  $\tau_b$  because of monotonic changes in the actual intensity level. On the other hand, decreasing  $\tau_0$  always reduces the deviation regardless of the value of  $\tau_b$ . However, this is not the only consideration for choosing an optimal value of  $\tau_0$ , because setting  $\tau_0$  too small artificially suppresses the SEP intensity increase recorded by this automated system.

[21] To determine an appropriate value of  $\tau_0$ , we consider the intensity suppression at the nine GLE events

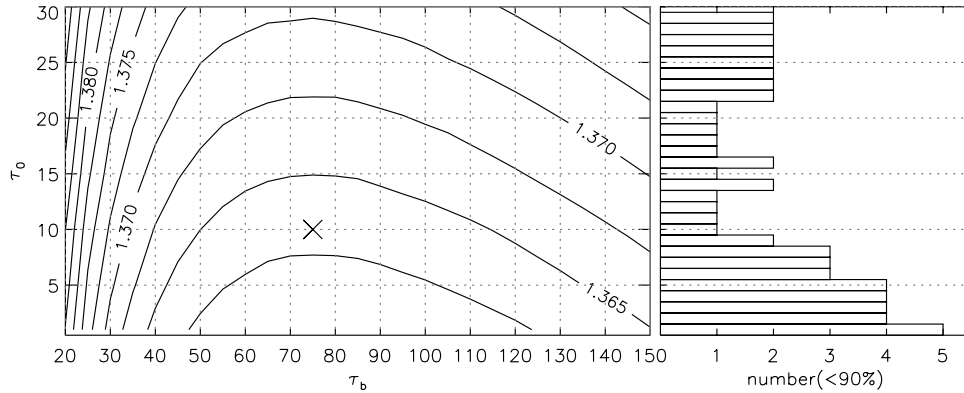


**Figure A1.** (left) Standard deviation of the cosmic ray intensity  $I(\tau)$  about the two parameters  $\tau_b$  and  $\tau_0$ . (right) Number of data points for which intensity is reduced to 90% or less of the correct (fixed baseline) value at the evaluation point.

listed in Table 2 as well as the standard deviation. As an example, the left plot of Figure A2 shows the intensity variation of the South Pole neutron monitor during the 26 December 2001 GLE event. The black line shows the intensity variation derived from a baseline defined by a 75 min average fixed before event onset. Colored lines show the intensity variation derived from equation (1) for  $\tau_0 = 1$  min (red),  $\tau_0 = 10$  min (blue), and  $\tau_0 = 20$  min (green) with  $\tau_b = 75$  min. It is clear that small  $\tau_0$  suppresses the intensity increase. Next, we examine the relation between the parameter  $\tau_0$  and the intensity suppression at all stations in nine GLE events. Evaluation points for this

examination are chosen at times where the intensity increase exceeds 5% for the first time. There are 47 intensity increases satisfying this condition. The right plot of Figure A2 shows the relationship between suppressed intensity and actual intensity at the evaluation time. The horizontal axis shows the intensity derived from the fixed baseline, while the vertical axis shows the intensity derived from equation (1) for  $\tau_0 = 1$  min (red) and  $\tau_0 = 10$  min (blue) with  $\tau_b = 75$  min. While blue points are concentrated on the solid line where the two intensities are the same, nearly all red points lie under this line. The number of data points that fall below the 90% level of suppressed

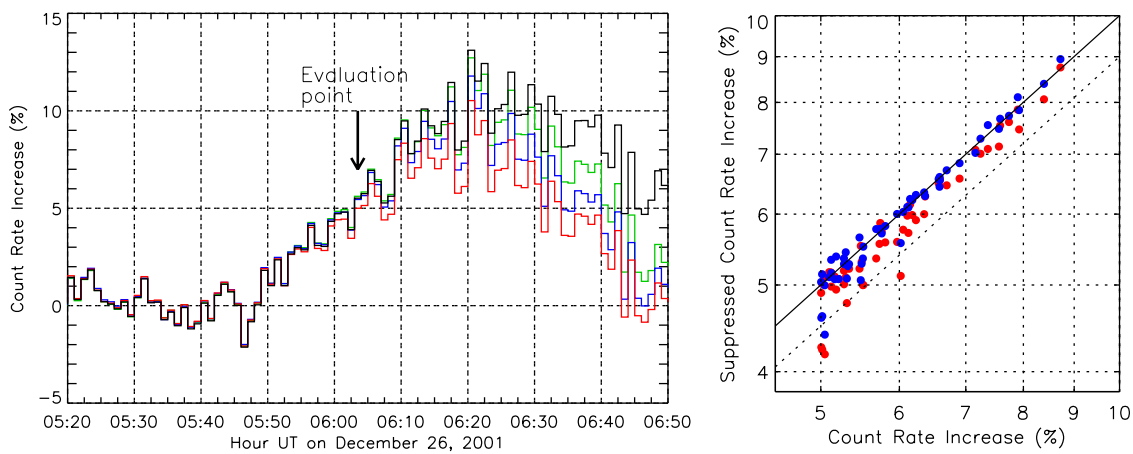


**Figure A2.** (left) Count rate increase of the South Pole neutron monitor during the GLE of 26 December 2001. Black line shows the intensity variation derived from a baseline defined as the 75 min average fixed before event onset. Colored lines show the intensity derived from equation (1) for  $\tau_0 = 1$  min (red),  $\tau_0 = 10$  min (blue), and  $\tau_0 = 20$  min (green) with  $\tau_b = 75$  min. (right) Comparison of the suppressed intensity with the actual intensity at the evaluation point (data point at which intensity increase first exceeds 5%). Horizontal axis is the intensity derived from a fixed baseline. Vertical axis is the suppressed intensity derived from equation (1) for a moving baseline with  $\tau_0 = 1$  min (red) and  $\tau_0 = 10$  min (blue) at  $\tau_b = 75$  min.

intensity (dotted line in the right plot of Figure A2) are plotted for all  $\tau_0$  as the histogram in Figure A1. This number is larger when less than 10 min is selected for  $\tau_0$ . Considering both plots in Figure A1, we finally choose 10 min for the parameter  $\tau_{0r}$  and 75 min for  $\tau_{br}$  as denoted by the cross in Figure A1. The standard deviation with these parameters is 1.363%.

## A2. Define the Threshold

[22] In this subsection, we determine the threshold level  $I_{th}$  for cosmic ray intensity, as well as the averaging time  $\tau_c$  used for the calculation of the current count rate. Using past data, we also evaluate the false alarm rate and elapsed time from GLE onset to the issuance of an alarm. Listed in Table A1 are false alarm numbers for different averaging periods  $\tau_c$  and threshold levels  $I_{th}$ . Three levels of false alarm number are listed in the same cell, arranged from top to bottom: alert, warning, and watch. These values are calculated from data that was observed over 4.4 years ( $\sim 1600$  days) when data from more than three stations are available from October 2000 to May 2005. To calculate these false alarm numbers, issued alarms are called off 30 min after the time when intensity falls back below the threshold level, because otherwise our data tend to issue several false alarms during a short period, as the intensity fluctuates back and forth across the threshold level during the event decay. Listed in Table A2 is the elapsed time between GLE onset and alarm issuance, averaged over nine GLE events. GLE onset times are defined as the time when one of the stations intensity (1 min value) exceeds 3%.

[23] In order to achieve the characteristics listed in Table 3, we set the appropriate false alarm number as zero for alert, and some small number for warning during this period. Considering the figures presented in Tables A1 and A2,  $I_{th} = 4\%$  and  $\tau_c \geq 2$  min fulfill our purpose. Because the watch false alarm rate is very high when  $\tau_c = 2$  min is selected (almost one occurrence per

**Table A1.** False Alarm Number During the Past 4.4 Years<sup>a</sup>

$\tau_c$	1 min	2 min	3 min	4 min	5 min
	$I_{th} = 5\%$				
Alert	0	0	0	0	0
Warning	12	0	0	0	0
Watch	4640	153	29	9	3
	$I_{th} = 4\%$				
Alert	1	0	0	0	0
Warning	323	3	1	1	1
Watch	22003	1361	171	52	21
	$I_{th} = 3\%$				
Alert	382	7	1	1	1
Warning	10112	170	21	12	7
Watch	10286	16264	3053	751	249

<sup>a</sup>These numbers are listed for each averaging interval and intensity threshold. Three kinds of false alarm number are listed in each cell.

**Table A2.** Average Elapsed Times Between GLE Onset and Alarm<sup>a</sup>

$\tau_c$	1 min	2 min	3 min	4 min	5 min
	$I_{th} = 5\%$				
Alert	6.9	8.0	7.9	8.8	9.6
Warning	4.8	6.6	7.2	7.4	7.9
Watch	2.2	3.2	4.0	5.2	6.0
	$I_{th} = 4\%$				
Alert	5.3	5.8	7.1	7.4	7.8
Warning	3.4	4.9	5.2	5.8	6.7
Watch	0.8	1.9	2.9	3.4	3.9
	$I_{th} = 3\%$				
Alert	3.6	5.1	5.2	6.0	6.3
Warning	1.8	3.4	3.8	4.6	5.1
Watch	0.0	0.6	1.0	1.4	2.7

<sup>a</sup>Onset times are defined for each event as a time when one station's intensity (1 min value) exceeds the 3% intensity threshold.

day), we choose  $\tau_c = 3$  min. Average elapsed times between GLE onset and the alarm for these parameters is almost the same as for  $\tau_c = 1$  min and  $I_{th} = 5\%$ , but the false alarm number is greatly reduced by choosing 3 min as  $\tau_c$ . In this condition ( $\tau_c = 3$  min,  $I_{th} = 4\%$ ), watch events become 171, corresponding to about 40 alarms per year. Only one false warning alarm occurred during the large Forbush decrease in July 2004. In neutron monitors, strong anisotropy sometimes occurs during a Forbush decrease, for instance bidirectional streaming and  $B \times \nabla n$  streaming [Kuwabara *et al.*, 2006]. However, the amplitude of these anisotropies is usually smaller than 4%, and the July 2004 event was a rare exception.

[24] **Acknowledgments.** The authors gratefully acknowledge the NOAA Space Environment Center and GOES team for providing useful space weather information. This work is supported in part by U.S. NSF grants ATM-0207196 and ATM-0527878.

## References

- Bieber, J. W., J. Clem, P. Evenson, R. Pyle, D. Ruffolo, and A. Saiz (2004), Spaceship Earth observations of the Easter 2001 solar particle event, *Astrophys. J.*, 601, L103–L106.
- Dorman, L., L. Pustil'nik, A. Sternlieb, and I. Zukerman (2003), Using ground-level cosmic ray observations for automatically generating predictions of hazardous energetic particle levels, *Adv. Space Res.*, 31, 847–852.
- Kuwabara, T., *et al.* (2006), Real-time cosmic ray monitoring system for space weather, *Space Weather*, 4, S08001, doi:10.1029/2005SW000204.
- Wilson, J. W., P. Goldhagen, V. Rafnsson, J. M. Clem, G. De Angelis, and W. Friedberg (2003), Overview of atmospheric ionizing radiation (AIR) research: SST – present, *Adv. Space Res.*, 32, 3–16.

J. W. Bieber, J. Clem, P. Evenson, T. Kuwabara, and R. Pyle, Bartol Research Institute and Department of Physics and Astronomy, University of Delaware, Newark, DE 19716, USA. (john@bartol.udel.edu; clem@bartol.udel.edu; penguin@bartol.udel.edu; takao@bartol.udel.edu; pyle@bartol.udel.edu)